Brief Definitive Report

Increased Severity of Local and Systemic Anaphylactic Reactions in gp49B1-deficient Mice

Massoud Daheshia,[1, 3] Daniel S. Friend,[1, 3] Michael J. Grusby,[1, 2] K. Frank Austen,[1, 3] and Howard R. Katz[1, 3]

[1]*Department of Medicine, Harvard Medical School, the* [2]*Department of Immunology and Infectious Disease, Harvard School of Public Health, and the* [3]*Division of Rheumatology, Immunology and Allergy, Brigham and Women's Hospital, Boston, MA 02115*

Abstract

gp49B1 is an immunoglobulin (Ig) superfamily member that inhibits FcεRI-induced mast cell activation when the two receptors are coligated with antibodies in vitro. The critical question of in vivo function of gp49B1 is now addressed in gene-disrupted mice. gp49B1-deficient mice exhibited a significantly increased sensitivity to IgE-dependent passive cutaneous anaphylaxis as assessed by greater tissue swelling and mast cell degranulation in situ. Importantly, by the same criteria, the absence of gp49B1 also resulted in a lower threshold for antigen challenge in active cutaneous anaphylaxis, in which the antigen-specific antibody levels were comparable in gp49B1-deficient and sufficient mice. Moreover, the absence of gp49B1 resulted in a significantly greater and faster death rate in active systemic anaphylaxis. These results indicate that gp49B1 innately dampens adaptive immediate hypersensitivity responses by suppressing mast cell activation in vivo. In addition, this study provides a new concept and target for regulation of allergic disease susceptibility and severity.

Key words: mast cells • immunoreceptor tyrosine-based inhibitory motif • passive cutaneous anaphylaxis • active cutaneous anaphylaxis • active systemic anaphylaxis

Introduction

Gp49B1 is a member of the Ig superfamily with two extracellular C2-type domains (1, 2) and two cytosolic immunoreceptor tyrosine-based inhibitory motifs (ITIMs) (3). This transmembrane receptor is expressed on mast cells (4), macrophages (5, 6), and cytokine- or virally stimulated NK cells (7–9). Gp49B1 is encoded by the *gp49B* gene (2), whereas the highly homologous *gp49A* gene (10) encodes the gp49A protein that does not have an ITIM (1) and, like gp49B1, is expressed in higher amounts on immature bone marrow–derived mast cell (BMMC) progenitors than on mature peritoneal mast cells (4, 10). Ab-mediated coligation of gp49B1 to FcεRI inhibits IgE-induced mast cell activation in vitro (3) by a mechanism requiring the ITIM tyrosines of gp49B1 and the src homology domain 2–containing phosphatase (SHP)-1 (11).

The ITIM was first identified in FcγRIIB (12, 13), whose extracellular domain is only distantly related to gp49B1 (3). FcγRIIB also differs because its ITIM inhibits cell activation through the recruitment of a src homology domain 2–containing inositol polyphosphate 5-phosphatase (SHIP) (14). FcγRIIB is widely expressed in the immune system, including on B cells and mast cells, and inhibits cell activation signaled by the B cell receptor and FcεRI in vitro (12, 13). FcγRIIB-deficient mice exhibit increased vascular permeability in IgG-dependent passive cutaneous anaphylaxis (PCA) (15) and a higher death rate during IgG- or IgE-dependent passive systemic anaphylaxis compared with normal mice (16). Because both IgE- and IgG-antigen complexes bind FcγRIIB (17), the increase in sensitivity of the deficient mice to anaphylactic reactions reflects the loss of direct feedback counterregulation during adaptive immediate hypersensitivity reactions.

The gp49 family is homologous with other families of activating and inhibitory receptors of the Ig superfamily that have C-2 type domains and are expressed on various cell types in the immune system. The inhibitory members of the human killer cell Ig-like receptor (KIR), leukocyte Ig-like receptor (LIR), and mouse paired Ig-like receptor (PIR) families share with gp49B1 the expression of ITIMs that recruit SHP-1 (for reviews, see references 18–20). The ligands for KIRs and two of the LIRs are polymorphic MHC class I molecules, and the binding of autologous class I by the receptors provides self-recognition that counter-

Address correspondence to Howard R. Katz, Division of Rheumatology, Immunology and Allergy, Brigham and Women's Hospital, 1 Jimmy Fund Way, Rm. 638A, Boston, MA 02115. Phone: 617-525-1307; Fax: 617-525-1308; E-mail: hrkatz@mbcrr.harvard.edu

regulates inappropriate activation signals. The ligands for the PIRs and most of the LIRs are unknown.

We recently identified the integrin αvβ3 as a functional ligand for gp49B1 in vitro (21). αvβ3 is widely distributed in vivo, being expressed on endothelial cells, fibroblasts, epithelial cells, and certain hematopoietic lineage cells (for a review, see reference 22). However, before addressing the ligand in vivo, it was critical to determine whether the absence of gp49B1 provided a mast cell phenotype with increased sensitivity to FcεRI-mediated, antigen-specific activation. We therefore generated mice with a targeted disruption of the *gp49B* gene and focused on the effects of gp49B1 deficiency on local and systemic anaphylactic reactions that have a major mast cell component. In PCA with defined IgE inputs, *gp49B*$^{-/-}$ mice showed markedly greater and prolonged tissue swelling concomitant with a more extensive degranulation of tissue mast cells compared with *gp49B*$^{+/+}$ mice. The increase in tissue swelling and the accelerated and greater rate of anaphylactic death in active cutaneous and systemic anaphylaxis, respectively, in gp49B-deficient mice, establishes for the first time the capacity of an ITIM-bearing receptor to attenuate active immediate hypersensitivity reactions. Thus, our results recognize a hyperresponsive mast cell phenotype in *gp49B*$^{-/-}$ mice, which in normal mice is dynamically counterregulated by the interaction of gp49B1 with innate tissue elements.

Materials and Methods

Generation of gp49B$^{-/-}$ *Mice.* A 6.4-kb 129/Sv EcoRI→HindIII genomic fragment containing the *gp49B* gene was subcloned into a modified pBluescript vector that had a thymidine kinase gene on the 3′ end. The region between the NcoI sites in intron 2 and exon 3 of the gp49B gene (2) was excised and replaced with the pMC1neo vector in the forward orientation (see Fig. 1 A). The targeting construct was transfected by electroporation into 129/Sv embryonic stem (ES) cells, and cells were selected with G418 and gancyclovir. To confirm homologous recombination, genomic DNA was extracted from the drug-selected cells, digested with SphI, and hybridized with a HindIII→SphI probe common to the 3′ regions of the *gp49A* and *gp49B* genes (see Fig. 1 A). The probe was predicted to hybridize with a 4.8-kb band reflecting the disrupted gp49B gene and with an ~9.5-kb band from the wild-type gp49B gene. All the clones had a 3.6-kb fragment from the wild-type gp49A gene, which has an SphI site in intron 5 that is not present in the gp49B gene (10). When the same blots were hybridized with an XhoI→SalI pMC1Neo probe, the clones that showed disruption of the gp49B gene with the HindIII→SphI probe demonstrated ~5.8- and 4.8-kb bands consistent with the gene disruption (data not shown). Moreover, there were no bands indicative of unintentional disruption of the gp49A gene. One of the clones with a disrupted *gp49B* gene (no. 69) was injected into BALB/c blastocysts, and chimeric mice were generated and crossed with BALB/c mice to produce male and female *gp49B*$^{+/-}$ mice. Those mice were intercrossed to yield *gp49B*$^{+/+}$, *gp49B*$^{+/-}$, and *gp49B*$^{-/-}$ mice (see Fig. 1 B). The homozygous mice on the 129/Sv × BALB/c background were then bred to yield *gp49B*$^{+/+}$ and *gp49B*$^{-/-}$ mice for study. All animal studies were approved by the Animal Care and Use Committee of the Dana-Farber Cancer Institute.

Culture of BMMC. Bone marrow cells from *gp49B*$^{+/+}$ and *gp49B*$^{-/-}$ mice were cultured for 3–8 wk in enriched medium containing 50% WEHI-3 cell (American Type Culture Collection) conditioned medium as described (3). After 3 wk, >97% of the nonadherent cells in the cultures were mast cells as assessed by metachromatic staining with toluidine blue.

Flow Cytometry. Cells (2.5×10^5) were incubated in 25 μl of calcium- and magnesium-free HBSS supplemented with 0.1% BSA and 0.02% sodium azide (HBA) alone or with saturating amounts of either rat mAb B23.1 (3) or rabbit anti-gp49$_{201–216}$ (10) for 30 min at 4°C. Cells were washed with HBA, incubated for 30 min at 4°C with FITC-labeled, F(ab′)$_2$ fragments of either goat IgG anti–rat IgM or goat anti–rabbit IgG-Fc (Jackson ImmunoResearch Laboratories) as appropriate for the first Ab, and washed again with HBA. Cells were resuspended in 2% paraformaldehyde in HBSS and analyzed on a Becton Dickinson FACSort™ using logarithmic fluorescence amplification.

PCA. The left and right ears of mice were injected intradermally with 20 μl of saline alone or containing 25 or 2.5 ng of mouse monoclonal IgE anti-DNP (clone SPE-7; Sigma-Aldrich), respectively. 20 h later, the mice were challenged with a 100 μl intravenous injection containing 100 μg of DNP-human serum albumin (HSA; Sigma-Aldrich), and ear thickness measurements were made with a caliper (Dyer Company). Net ear swelling was calculated as the difference between the thicknesses of the right and left ears of each mouse.

Active Cutaneous and Systemic Anaphylaxis. Mice were immunized intraperitoneally on days 0 and 5 with 10 μg of chicken OVA adsorbed to 1 mg of alum. Approximately 3 wk after the initial injection, the left and right ears of mice were injected intradermally with 20 μl of saline alone or containing 50 ng OVA, respectively. Net ear swelling was calculated as for PCA. For systemic anaphylaxis, immunized mice were injected intravenously with 10 mg of OVA in 100 μl of PBS. The outcome was quantified by the number of animals dying and the time to death.

Histology. Ears were excised, fixed in 4% paraformaldehyde for at least 8 h, and embedded in glycolmethacrylate. Sections (2 μm) were placed on slides, air dried, and stained for 20 s in a 5% ethanolic solution of toluidine blue or in Diff-Quik (Dade Behring, Inc.). For enumeration of intact mast cells, 10 high power fields (50× objective) of each ear were examined on a Leica Dialux 20 microscope.

Statistical Analyses. Significance was assessed with Student's unpaired, two-tailed *t* test. *P* values < 0.05 were considered to be significant.

Results and Discussion

Generation of gp49B$^{-/-}$ *Mice.* ES cells (129/Sv strain) were transfected with a targeting construct that had a pMc1Neo construct replacing a region of the *gp49B* gene running from intron 2 through most of exon 3 (that encodes the NH_2-terminal Ig-like domain; Fig. 1 A). Of 104 G418- and gancyclovir-resistant clones, 2 had a disrupted *gp49B* gene by Southern blot analyses. A clone was microinjected into blastocysts from BALB/c mice to generate chimeric mice, which were bred to BALB/c mice to produce heterozygotes that were then intercrossed to yield *gp49B*$^{+/+}$, *gp49B*$^{+/-}$, and *gp49B*$^{-/-}$ mice (Fig. 1 B). *gp49B*$^{-/-}$ mice were fertile, had litters of normal size, and remained healthy when living in a viral Ab-free, barrier vi-

varium. Similarly, naive *gp49B*$^{-/-}$ mice in a mixed 129 × C57BL/6 background were reported to be normal for these characteristics (23).

The expression of gp49B1 and gp49A proteins was assessed on BMMCs from *gp49B*$^{+/+}$ and *gp49B*$^{-/-}$ mice. The gp49B1-specific mAb B23.1 (3) bound to BMMCs generated from *gp49B*$^{+/+}$, but not *gp49B*$^{-/-}$ mice (Fig. 1 C). gp49A-specific anti-gp49$_{201–216}$ (10) bound equivalently to BMMCs from *gp49B*$^{+/+}$ and *gp49B*$^{-/-}$ mice. In addition, peritoneal mast cells from *gp49B*$^{-/-}$ mice did not bind mAb B23.1, as assessed by two-color flow cytometry using anti–c-kit to identify mast cells (data not shown). Hence, the gp49B gene product was specifically absent in cells from *gp49B*$^{-/-}$ mice. These results also confirm our previous conclusion, based on flow cytometric analyses of gp49A and gp49B transfectants, that mAb B23.1 is gp49B1-specific (3).

Effects of gp49B1 Deficiency on PCA. To determine whether gp49B1 regulates FcεRI-mediated mast cell activation in vivo, we tested the effects of gp49B1 deficiency on the IgE-mediated PCA reaction in the ear. Passive sensitization with a defined input of IgE assures that subsequent antigen challenge is directed to the mast cells (24) and avoids the variation in titers of Ab classes that can occur with active sensitization. The left and right ears of mice were injected intradermally with saline or monoclonal IgE anti-DNP, respectively. 20 h later, the mice were challenged with an intravenous injection of DNP-HSA (100 μg), and initial measurements were made 0.5 h later, a time that falls within the 15 to 45 min plateau of the peak response (25). The net swelling in the ears of *gp49B*$^{+/+}$ mice declined progressively from the 0.5 h time point and was essentially undetectable by 4 h (Fig. 2 A). The sensitized ears of *gp49B*$^{-/-}$ mice showed two- to threefold greater net swelling at 0.5 to 2 h after challenge compared with *gp49B*$^{+/+}$ mice, and also declined progressively from the 0.5 h peak response with barely detectable swelling at 4 and 8 h. Enhanced swelling in the ears of the deficient mice was also evident histologically 0.5 h after challenge and was due to separation of the structural elements by edema, which had largely subsided in both genotypes by 4 h (Fig. 2 B). There was no influx of neutrophils, eosinophils, or other cell types evident within the time frame for the net tissue swelling. Importantly, the number of morphologically intact mast cells, defined as cells with metachromatic granules associated with a nucleus, was a significant twofold lower at both 0.5 and 4 h after challenge of *gp49B*$^{-/-}$ mice (Fig. 2 C), indicative of an enhanced susceptibility to mast cell degranulation in the deficient animals.

To determine whether this augmented mast cell response reflected a reduced requirement for the concentration of sensitizing IgE, the PCA reaction was conducted with an

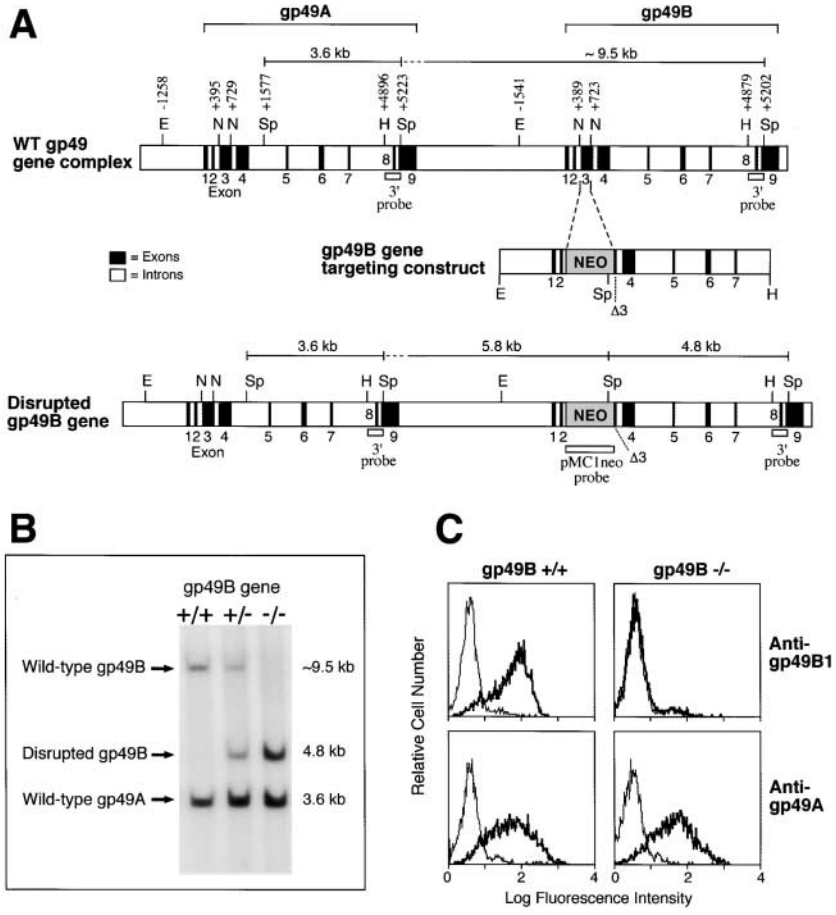

Figure 1. Generation of *gp49B*$^{-/-}$ mice. (A) Genomic organization of the mouse *gp49A* and *gp49B* genes (top), structure of the targeting vector (middle), and organization of the disrupted allele. The expected fragment sizes of 3.6, ~9.5, and 4.8 kb for the wild-type (WT) gp49A, WT gp49B, and disrupted gp49B genes, respectively, in the blot analysis in B are indicated by brackets. E, EcoRI; N, NcoI; Sp, SphI; H, HindIII; Δ3, truncated exon 3. (B) DNA blot analysis of SphI-digested genomic DNA identifying *gp49B*$^{+/+}$, *gp49B*$^{+/-}$, and *gp49B*$^{-/-}$ mice by hybridization with a HindIII→SphI gp49A/gp49B1 genomic fragment to provide the fragment sizes defined in panel A. (C) Flow cytometric analysis of BMMCs from *gp49B*$^{+/+}$ and *gp49B*$^{-/-}$ mice stained with mAb B23.1 (anti-gp49B1; top panels, thick lines) or polyclonal anti-gp49$_{201–216}$ (anti-gp49A; bottom panels, thick lines) and the respective negative controls (thin lines).

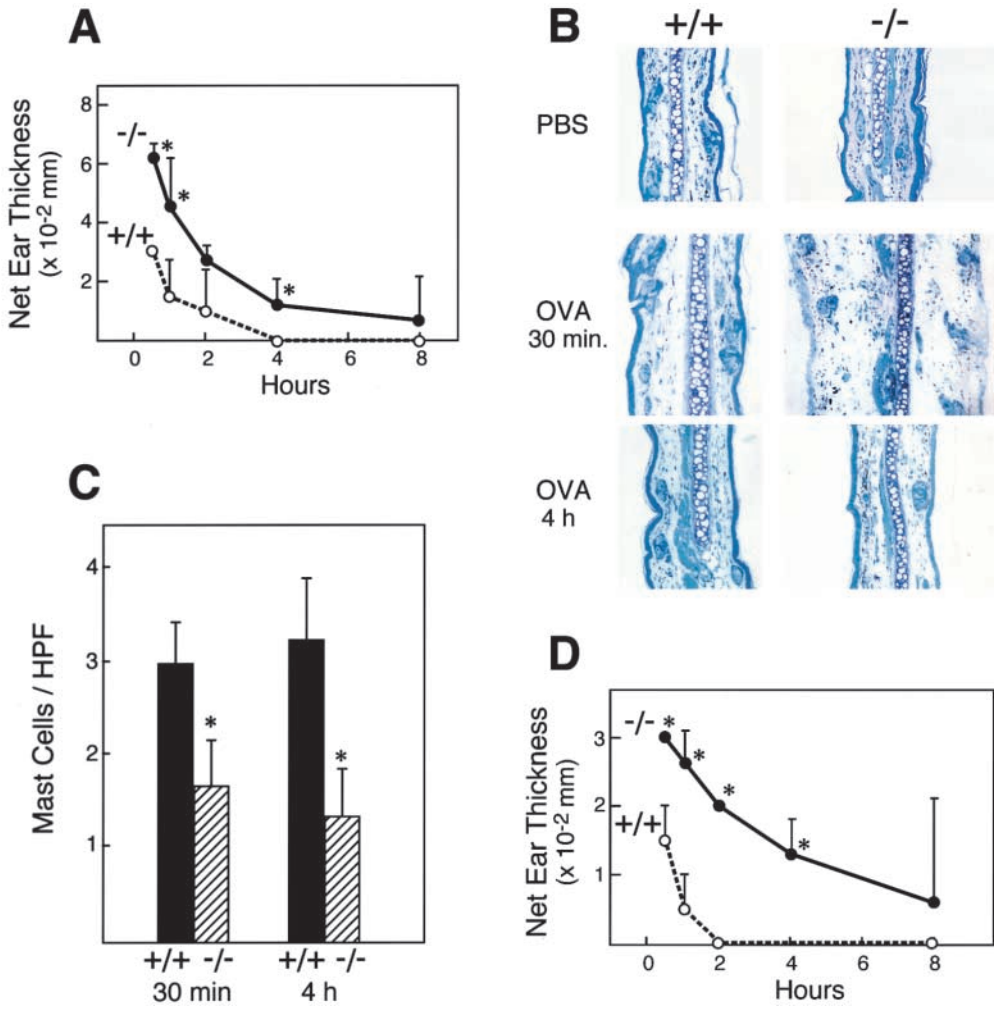

Figure 2. Effects of gp49B1 deficiency on PCA assessed by ear swelling and histology. Mice were injected intradermally with 20 μl of saline alone (left ears) or containing 25 (A–C) or 2.5 (D) ng of mouse monoclonal IgE anti-DNP (right ears). After 20 h, the mice were injected intravenously with 100 μg of DNP-HSA in 100 μl of PBS. (A and D) Time course of net ear swelling (right ear minus left ear) measured with a thickness caliper. Data are expressed as mean ± SD, $n = 4$. (B) Diff-Quik–stained tissue sections of control and challenged ears (control ears obtained from mice not injected with IgE); original magnification: 10×. (C) Quantification of intact mast cells, defined as having metachromatic cytoplasmic granules surrounding an intact nucleus, per high power field (HPF) in tissue sections from the ears of $gp49B^{+/+}$ (black bars) and $gp49B^{-/-}$ (hatched bars) mice 0.5 and 4 h, respectively, after antigen challenge. Data are expressed as mean ± SD, $n = 3$. $^*P < 0.05$ compared with $gp49B^{+/+}$ mice.

intradermal injection of 2.5 ng of IgE, a dose that is 10- to 100-fold lower than is customarily used (24, 26). In $gp49B^{+/+}$ mice, maximal swelling at 0.5 h was one-half that obtained with 25 ng of IgE and was undetectable beyond 1 h (Fig. 2 D). The ear swelling in $gp49B^{-/-}$ mice was also lower than that observed with the higher IgE dose, but was dramatically greater than that of $gp49B^{+/+}$ mice at the low IgE dose (Fig. 2 D). Furthermore, the magnitude of the ear swelling in $gp49B^{-/-}$ mice with low dose IgE sensitization was equivalent to that of $gp49B^{+/+}$ mice sensitized with 10-fold more IgE. Thus, the $gp49B^{-/-}$ mouse has an elicited phenotype of enhanced susceptibility to IgE-mediated mast cell activation over a 10-fold range of IgE sensitizing concentrations in situ. Inasmuch as the rapid and edematous tissue swelling in PCA is mast cell dependent (24), our findings establish conclusively that gp49B1 is an endogenous inhibitor of IgE-mediated mast cell activation in vivo. The observation of others that IgE-initiated degranulation of BMMC from $gp49B^{-/-}$ and $gp49B^{+/+}$ mice is comparable in vitro (23) could be explained by the absence of a tissue ligand for gp49B1 in those cell suspensions.

Recently, mice deficient in leukotriene (LT)C_4 synthase were found to exhibit attenuated ear swelling in IgE-dependent PCA (25), revealing a previously unappreciated contribution of mast cell–derived LTC_4 and its receptor-active metabolites in immediate tissue swelling. PCA with 50 ng IgE was attenuated in LTC_4 synthase-deficient mice by 50% compared with normal littermates (25), indicating that the cysteinyl leukotrienes are as significant as the amine mediators exocytosed from mast cell secretory granules in terms of the induction of early edema. Because coligation of gp49B1 with cross-linked FcεRI inhibits the generation of LTC_4 by mast cells in vitro (3), it seems likely that the augmented production of cysteinyl leukotrienes and/or their synergistic action with the released amines contributes to the increase in PCA-associated tissue swelling in $gp49B^{-/-}$ mice.

Effects of gp49B1-deficiency on Acute Active Cutaneous Anaphylaxis. To more fully assess the biologic relevance of gp49B1 in the negative regulation of immediate hypersensitivity, we used a model of active cutaneous anaphylaxis. OVA-immunized $gp49B^{+/+}$ mice that were challenged intradermally in the ear with 50 ng of antigen demonstrated little tissue swelling as measured by micrometry (Fig. 3 A) or histology (Fig. 3 B), despite an antigen-specific Ab response (Table I). In striking contrast, $gp49B^{-/-}$ mice with a

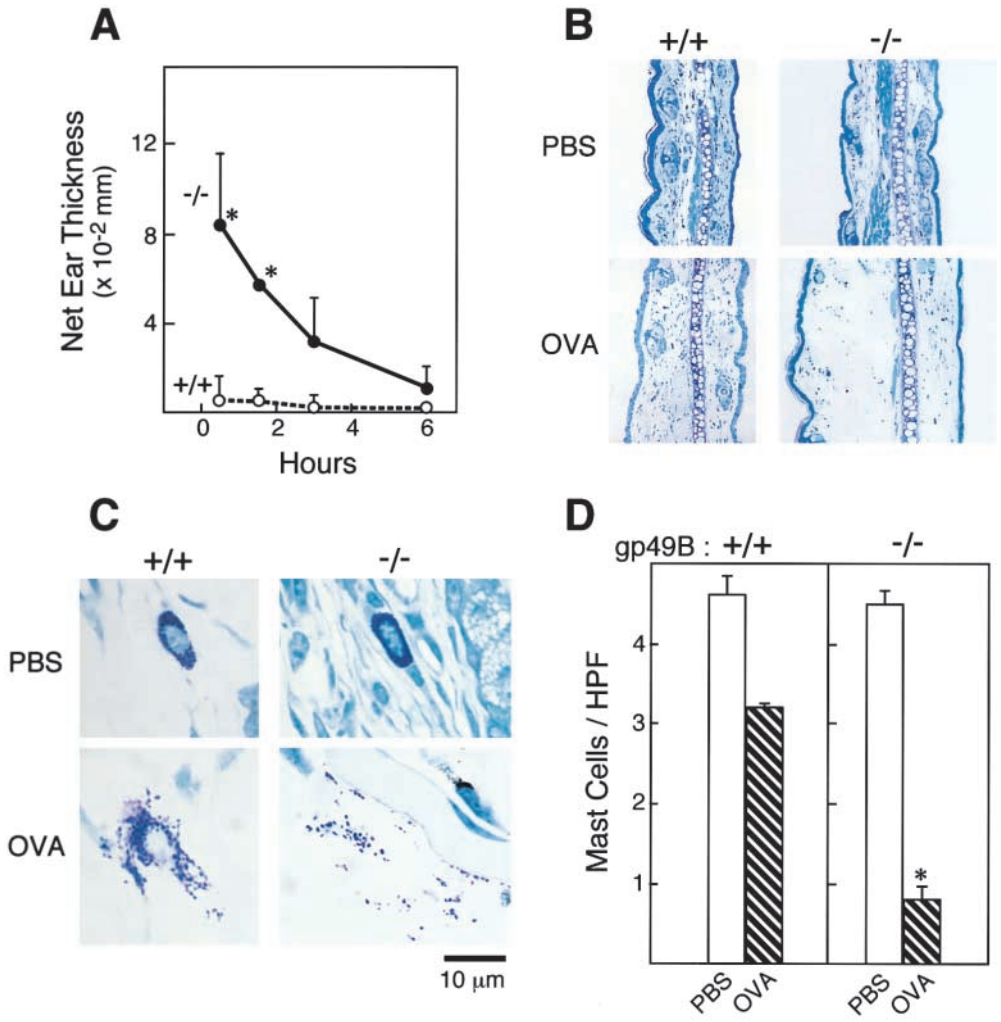

Figure 3. Effects of gp49B1 deficiency on active cutaneous anaphylaxis. Mice were injected on day 0 and 5 with 10 μg of OVA adsorbed to 1 mg of alum. Three wk after the initial injection, the left and right ears of mice were injected intradermally with 20 μl of saline alone or containing 50 ng OVA, respectively. (A) Time course of net ear swelling measured as described in the legend to Fig. 2. Data are expressed as mean ± SD, $n = 3$. (B) Diff-Quik–stained tissue sections of control and challenged ears 0.5 h after intradermal injection; original magnification: 10×. (C) Higher magnification (100× objective) of tissue sections represented in B showing intact and degranulated mast cells. (D) Quantification of intact mast cells in tissue sections from ears 0.5 h after injection with PBS (white bars) or OVA (hatched bars), measured as described in the legend to Fig. 2. Data are expressed as mean ± SD, $n = 3$. $^*P < 0.05$ compared with $gp49B^{+/+}$ mice.

comparable Ab response showed robust swelling at 0.5 h that was somewhat greater than that obtained by PCA with 25 ng of hapten-specific IgE (Fig. 2 A), and which consisted of edema without a cellular infiltrate (Fig. 3 B). The challenged ears of $gp49B^{-/-}$ mice showed fourfold fewer intact mast cells 0.5 h after challenge compared with $gp49B^{+/+}$ mice as noted histologically (Fig. 3 C) and quantified by cell counting (Fig. 3 D).

Whereas the contribution of mast cells to early tissue swelling in active anaphylaxis in mice has not been formally established, the decrease in intact mast cells 0.5 h after intradermal antigen challenge of immunized gp49B1-deficient mice (Fig. 3 C) suggests that a concomitant, augmented release of vasoactive mediators from mast cells accounts for the tissue edema (Fig. 3 B). Moreover, the findings indicate that the absence of gp49B1 augments the effector phase of a polyclonal, acquired immune response that likely involves mast cell activation through both IgE/FcεRI and IgG/FcγRIII.

Effect of gp49B1 Deficiency on Active Systemic Anaphylaxis. Mice immunized with OVA were injected intravenously with 10 mg OVA. Initial observations suggested that $gp49B^{-/-}$ mice became moribund more frequently and rapidly than normal animals, so the outcome was quantified in additional experiments. Whereas 8 out of 29 (27%) $gp49B^{+/+}$ mice died in response to systemic antigen challenge, 17 out of 25 (68%) $gp49B^{-/-}$ mice died. Moreover, the mean times to death were 45 ± 9 and 26 ± 8 min in $gp49B^{+/+}$ and $gp49B^{-/-}$ mice, respectively, which were significantly different ($P < 0.0001$). In two out of three $gp49B^{-/-}$ mice that died, the lungs showed focal leukose-

Table I. *OVA-specific Serum Ig Levels at Day 20 in Immunized $gp49B^{+/+}$ and $gp49B^{-/-}$ Mice*

	$gp49B^{+/+}$	$gp49B^{-/-}$
IgG	122 ± 71	134 ± 112
IgG1	251 ± 199	222 ± 189
IgG2a	924 ± 1,470	954 ± 893
IgM	0.172 ± 0.105	0.199 ± 0.036
IgE	151 ± 149	101 ± 66

Data are expressed as mean ng/ml ± SD ($n = 8$).

questration of neutrophils and mast cells had degranulated in the trachea. In the heart, myocyte swelling with distorted myofibrils was associated with mast cell degranulation. Mast cell degranulation was not seen in three *gp49B*$^{+/+}$ mice at the interval by which the *gp49B*$^{-/-}$ mice died.

That the mast cell can be responsible for a fatal outcome has been established in passive models using anti-IgE or IgE sensitization followed by antigen, in which death occurs within 40 to 60 min in WBB6F1-+/+ mice, but mast cell–deficient WBB6F1-W/W^{v} mice survive (27–29). In active systemic anaphylaxis with these two strains of mice, the mast cell contribution was most evident for the cardiac tachycardia, and death was not dependent on the mast cell, thus reflecting other pathways (27, 28). Hence, while the mast cell may not be the absolute cause of death in *gp49B*$^{-/-}$ mice, the susceptibility of the *gp49B*$^{-/-}$ mice to fatal active systemic anaphylaxis in a relatively short interval compared with *gp49B*$^{+/+}$ mice is compatible with an augmented burst of mediator release from mast cells.

In summary, our results establish that gp49B1 is an inhibitor of FcϵRI-directed mast cell activation and attendant immediate hypersensitivity reactions in vivo. This constitutive effect of gp49B1 is sufficiently robust to attenuate the local and systemic anaphylactic effects of antigen challenge during an ongoing immune response. Thus, tissue mast cells through their expression of gp49B1 possess an innate system that counterregulates acquired allergic inflammation.

Supported by National Institutes of Health grants AI07306, AI22531, AI31599, AI40171, AI41144, and HL36110; and by a grant from the Mathers Foundation. M.J. Grusby is a Scholar of the Leukemia and Lymphoma Foundation.

Submitted: 23 May 2001
Accepted: 11 June 2001

References

1. Arm, J.P., M.F. Gurish, D.S. Reynolds, H.C. Scott, C.S. Gartner, K.F. Austen, and H.R. Katz. 1991. Molecular cloning of gp49, a cell surface antigen that is preferentially expressed by mouse mast cell progenitors and is a new member of the immunoglobulin superfamily. *J. Biol. Chem.* 266: 15966–15973.
2. Castells, M.C., X. Wu, J.P. Arm, K.F. Austen, and H.R. Katz. 1994. Cloning of the gp49B gene of the immunoglobulin superfamily and demonstration that one of its two products is an early-expressed mast cell surface protein originally described as gp49. *J. Biol. Chem.* 269:8393–8401.
3. Katz, H.R., E. Vivier, M.C. Castells, M.J. McCormick, J.M. Chambers, and K.F. Austen. 1996. Mouse mast cell gp49B1 contains two immunoreceptor tyrosine-based inhibition motifs and suppresses mast cell activation when coligated with the high-affinity Fc receptor for IgE. *Proc. Natl. Acad. Sci. USA.* 93:10809–10814.
4. Katz, H.R., A.C. Benson, and K.F. Austen. 1989. Activation- and phorbol ester-stimulated phosphorylation of a plasma membrane glycoprotein antigen expressed on mouse IL-3-dependent mast cells and serosal mast cells. *J. Immunol.* 142:919–926.
5. LeBlanc, P.A., and C.A. Biron. 1984. Mononuclear phagocyte maturation: a cytotoxic monoclonal antibody reactive with postmonoblast stages. *Cell. Immunol.* 83:242–254.
6. Matsumoto, Y., L.L. Wang, W.M. Yokoyama, and T. Aso. 2001. Uterine macrophages express the gp49B inhibitory receptor in midgestation. *J. Immunol.* 166:781–786.
7. Rojo, S., D.N. Burshtyn, E.O. Long, and N. Wagtmann. 1997. Type I transmembrane receptor with inhibitory function in mouse mast cells and NK cells. *J. Immunol.* 158:9–12.
8. Wang, L.L., I.K. Mehta, P.A. LeBlanc, and W.M. Yokoyama. 1997. Mouse natural killer cells express gp49B1, a structural homolog of human killer inhibitory receptors. *J. Immunol.* 158:13–17.
9. Wang, L.L., D.T. Chu, A.O. Dokun, and W.M. Yokoyama. 2000. Inducible expression of the gp49B inhibitory receptor on NK cells. *J. Immunol.* 164:5215–5220.
10. McCormick, M.J., M.C. Castells, K.F. Austen, and H.R. Katz. 1999. The gp49A gene has extensive sequence conservation with the gp49B gene and provides gp49A protein, a unique member of a large family of activating and inhibitory receptors of the immunoglobulin superfamily. *Immunogenetics.* 50:286–294.
11. Lu-Kuo, J.M., D.M. Joyal, K.F. Austen, and H.R. Katz. 1999. gp49B1 inhibits IgE-initiated mast cell activation through both immunoreceptor tyrosine-based inhibitory motifs, recruitment of the src homology 2 domain-containing phosphatase-1, and suppression of early and late calcium mobilization. *J. Biol. Chem.* 274:5791–5796.
12. Muta, T., T. Kurosaki, Z. Misulovin, M. Sanchez, M.C. Nussenzweig, and J.V. Ravetch. 1994. A 13-amino-acid motif in the cytoplasmic domain of FcγRIIB modulates B-cell receptor signalling. *Nature.* 368:70–73.
13. Daëron, M., S. Latour, O. Malbec, E. Espinosa, P. Pina, S. Pasmans, and W.H. Fridman. 1995. The same tyrosine-based inhibition motif, in the intracytoplasmic domain of FcγRIIB, regulates negatively BCR-, TCR-, and FcR-dependent cell activation. *Immunity.* 3:635–646.
14. Ono, M., S. Bolland, P. Tempst, and J.V. Ravetch. 1996. Role of the inositol phosphatase SHIP in negative regulation of the immune system by the receptor FcγRIIB. *Nature.* 383: 263–266.
15. Takai, T., M. Ono, M. Hikida, H. Ohmori, and J.V. Ravetch. 1996. Augmented humoral and anaphylactic responses in FcγRII-deficient mice. *Nature.* 379:346–349.
16. Ujike, A., Y. Ishikawa, M. Ono, T. Yuasa, T. Yoshino, M. Fukumoto, J.V. Ravetch, and T. Takai. 1999. Modulation of immunoglobulin (Ig) E-mediated systemic anaphylaxis by low-affinity Fc receptors for IgG. *J. Exp. Med.* 189:1573–1579.
17. Takizawa, F., M. Adamczewski, and J.-P. Kinet. 1992. Identification of the low affinity receptor for immunoglobulin E on mouse mast cells and macrophages as FcγRII and FcγRIII. *J. Exp. Med.* 176:469–476.
18. Lanier, L.L. 1998. Activating and inhibitory NK cell receptors. *Adv. Exp. Med. Biol.* 452:13–18.
19. Colonna, M., H. Nakajima, and M. Cella. 2000. A family of inhibitory and activating Ig-like receptors that modulate function of lymphoid and myeloid cells. *Semin. Immunol.* 12: 121–127.
20. Kubagawa, H., M.D. Cooper, C.C. Chen, L.H. Ho, T.L. Alley, V. Hurez, T. Tun, T. Uehara, T. Shimada, and P.D. Burrows. 1999. Paired immunoglobulin-like receptors of activating and inhibitory types. *Curr. Top. Microbiol. Immunol.* 244:137–149.

21. Castells, M.C., L.B. Klickstein, K. Hassani, J.A. Cumplido, M.E. Lacouture, K.F. Austen, and H.R. Katz. 2001. gp49B1-αvβ3 interaction inhibits antigen-induced mast cell activation. *Nat. Immunol.* 2:436–442.
22. Felding-Habermann, B., and D.A. Cheresh. 1993. Vitronectin and its receptors. *Curr. Opin. Cell Biol.* 5:864–868.
23. Rojo, S., C.C. Stebbins, M.E. Peterson, D. Dombrowicz, N. Wagtmann, and E.O. Long. 2000. Natural killer cells and mast cells from gp49B null mutant mice are functional. *Mol. Cell. Biol.* 20:7178–7182.
24. Wershil, B.K., Y.A. Mekori, T. Murakami, and S.J. Galli. 1987. ^{125}I-fibrin deposition in IgE-dependent immediate hypersensitivity reactions in mouse skin. Demonstration of the role of mast cells using genetically mast cell-deficient mice locally reconstituted with cultured mast cells. *J. Immunol.* 139:2605–2614.
25. Kanaoka, Y., A. Maekawa, J.F. Penrose, K.F. Austen, and B.K. Lam. 2001. Attenuated zymosan-induced peritoneal vascular permeability and IgE-dependent passive cutaneous anaphylaxis in mice lacking leukotriene C_4 synthase. *J. Biol. Chem.* 276:22608–22613.
26. Dombrowicz, D., V. Flamand, K.K. Brigman, B.H. Koller, and J.-P. Kinet. 1993. Abolition of anaphylaxis by targeted disruption of the high affinity immunoglobulin E receptor α chain gene. *Cell.* 75:969–976.
27. Takeishi, T., T.R. Martin, I.M. Katona, F.D. Finkelman, and S.J. Galli. 1991. Differences in the expression of the cardiopulmonary alterations associated with anti-immunoglobulin E-induced or active anaphylaxis in mast cell-deficient and normal mice. Mast cells are not required for the cardiopulmonary changes associated with certain fatal anaphylactic responses. *J. Clin. Invest.* 88:598–608.
28. Miyajima, I., D. Dombrowicz, T.R. Martin, J.V. Ravetch, J.P. Kinet, and S.J. Galli. 1997. Systemic anaphylaxis in the mouse can be mediated largely through IgG1 and FcγRIII. Assessment of the cardiopulmonary changes, mast cell degranulation, and death associated with active or IgE- or IgG1-dependent passive anaphylaxis. *J. Clin. Invest.* 99:901–914.
29. Martin, T.R., S.J. Galli, I.M. Katona, and J.M. Drazen. 1989. Role of mast cells in anaphylaxis. Evidence for the importance of mast cells in the cardiopulmonary alterations and death induced by anti-IgE in mice. *J. Clin. Invest.* 83:1375–1383.